Publ. Astron. Soc. Japan 39, 95–107 (1987)

The Magnetic Field near the Galactic Center

Yoshiaki SOFUE

*Nobeyama Radio Observatory,**
Minamimaki-mura, Minamisaku-gun, Nagano 384–13
and
Department of Astronomy, Faculty of Science, University of Tokyo, Bunkyo-ku, Tokyo 113

Wolfgang REICH

Max-Planck-Institut für Radioastronomie, Auf dem Hügel 69,
D-5300 Bonn 1, F.R.G.

Makoto INOUE

*Nobeyama Radio Observatory,**
Minamimaki-mura, Minamisaku-gun, Nagano 384–13

and

John H. SEIRADAKIS

Department of Astronomy, University of Thessaloniki,
GR-54006 Thessaloniki, Greece

(Received 1986 July 9; accepted 1986 September 8)

Abstract

Multichannel, narrow-band polarimetric observations at 5 GHz of the galactic center region have been made using the Effelsberg 100-m telescope. Polarization structures near the radio arc are basically consistent with previous 10-GHz observations, but there exists a significant discrepancy in position and rotation measure characteristics between 5 and 10 GHz for the polarized emission on the radio arc. This indicates a complicated internal Faraday rotation in the arc. The distributions of rotation measure across the galactic plane and across the rotation axis of the Galaxy suggest the existence of a large-scale poloidal magnetic field twisted by the disk rotation. A primordial origin is suggested for the poloidal field. Some polarization was found on the edges of the radio bridge, that connects the radio arc with Sgr A, and a Faraday rotation reaching $|\mathrm{RM}| \sim 10^3$ rad m^{-2} was recorded, whereas the bridge center is depolarized. This fact shows for the first time the magnetoionic characteristics of the radio bridge.

Key words: Faraday rotations; Galactic center; Linear polarization; Magnetic fields.

* Nobeyama Radio Observatory, a branch of the Tokyo Astronomical Observatory, University of Tokyo, is a facility open for general use by researchers in the field of astronomy, astrophysics, and astrochemistry.

1. Introduction

Linearly polarized radio emission has been detected near the galactic center along the radio arc (Brown and Liszt 1984) and its extension above and below the galactic plane (Inoue et al. 1984; Yusef-Zadeh et al. 1984, 1986; Tsuboi et al. 1985, 1986; Seiradakis et al. 1985). The polarized feature has three basic components: a compact source at G 0.16−0.15 on the radio arc (source A) and the northwestern (B) and southeastern (C) "plumes." The plumes are elongated, perpendicular to the galactic plane, extend up to $b=\pm 0^{\circ}.6$ and are symmetrically located with respect to source A. Source B coincides with the beginning of the eastern ridge of the Ω-shaped galactic center lobe (GCL: Sofue and Handa 1984; Sofue 1985).

Rotation measures (RM) and intrinsic polarization angles have been determined at 10 GHz along the polarized features (Tsuboi et al. 1986): A and C have negative RM as large as −1000 to −2000 rad m^{-2}, whereas B has a positive RM of up to 1000 rad m^{-2}. The intrinsic polarization angles show that the magnetic field is aligned parallel to the polarized features, or perpendicular to the galactic plane. The change of sign of RM indicates a reversal of the line-of-sight field from the upper to the lower sides of the galactic plane.

The polarization observations have provided a powerful tool to investigate the magnetic field in the central region of our Galaxy, which has long been hidden from our view because radiation traveling along the long path undergoes large Faraday depolarization at lower frequencies. In this paper we report new multichannel, narrow-band polarimetric measurements of the polarized features at 5 GHz using the Effelsberg 100-m telescope. We discuss a possible structure of a magnetic field in the central 50 pc of the Galaxy and report the first detection of the magnetic field along the radio bridge.

2. Observations and Results

(i) Observations

The observations were made on four successive nights from June 20 through 23, 1985 with the Effelsberg 100-m telescope. We mapped a region of $70' \times 40'$ square in extent centered on R.A.(1950)$=17^{h}43^{m}.0$, Decl.(1950)$=-28^{\circ}50'.0$. Each night we made three coverages, two by scanning in the right ascension direction and one in the declination direction. Scan separation and speed were $1'$ and 1° min^{-1}, respectively. The center frequency was changed each night, so that we observed at 4550, 4670, 4806, and 4950 MHz. The bandwidth of our observations was 40 MHz and the HPBW of the telescope was $2'.4$.

The data were calibrated by 3C 286 assuming a flux density of 7.5 Jy and linear polarization of 11.5% at polarization angle of 33°. The data at each frequency were combined to I, U, and Q maps after correction for scanning effects, interference etc. We found that the narrow-band instrumental polarization was about 1.2–1.5% at each frequency, which was substantially higher than that normally encountered in the 500-MHz broad-band response. This affects the polarization structure of the bridge and arc regions to some extent. We therefore corrected for the instrumental response of the U and Q maps by convolving the total intensity maps with the instrumental

response within 6′ of Sgr A West. The H II region Sgr B2 at the edge of the field does not show any polarization after the correction, indicating the success of our procedure. Furthermore, the U and Q instrumental characteristics vary drastically in an unsystematic way among the four channels. So we checked the corrected maps for polarized features of this kind, but found them not existing any more. The remaining instrumental response in the resultant maps is estimated to be less than 0.05%.

The narrow band enables us to detect the polarized intensity without suffering from Faraday depolarization within the bandwidth. The band depolarization can be ignored provided $|\mathrm{RM}| \leq 1/(2\lambda\Delta\lambda)$, or in our case when $|\mathrm{RM}| \leq 16000$ rad m^{-2}. Here RM is defined by $d\phi/d(\lambda^2)$, where ϕ and λ are the polarization angle and the wavelength, respectively. This may be compared with the band depolarization limit of $|\mathrm{RM}| \leq 11000$ rad m^{-2} in the case of the 10-GHz observations by Inoue et al. (1984). Also the small channel separation, 100 MHz, makes it possible to determine the RM from any two channels without the $n\pi$ ambiguity of the polarization angle provided $|\mathrm{RM}| \lesssim 6000$ rad m^{-2}. Using all four channels we get completely unambiguous results.

From the obtained I, Q, and U data, we obtain the polarization angle, degree of polarization, polarized intensity at each frequency channel, and those summed up over the four frequencies. The rms noise on the resultant I_p (polarized intensity) maps was about 10 mK T_b, which gives a typical error in the ϕ determination of $\Delta\phi \approx \pm 5°$ at $I_p \approx 50$-mK level. The RM determination has therefore an error of $\Delta\mathrm{RM} \cong \pm 200$ rad m^{-2}. This error in RM at 5 GHz causes an error in the intrinsic polarization angle of $\Delta\phi_0 \approx \pm 50°$. Hence the present data, except for a few peak positions, cannot be used to determine the field direction, but only give the RM distribution.

(ii) Total Intensity and Polarized Features

A total intensity map of the galactic center region at broad band 6 cm for a $1° \times 1°$ area was recently published by Seiradakis et al. (1985) as an image processed radiograph. We used this map for a base-level correction and finally combined over averaged total intensity maps with the broad-band map, which agrees quite well with each other. The resulting map is shown in figure 1.

Figure 2 shows the average polarized intensity distribution from the four channels

Table 1. Polarized properties along the radio arc at 5 and 10 GHz.*

Source	l	b	α (1950)	δ (1950)	Polarization degree (%)		RM (rad m^{-2})	
					5 GHz	10 GHz	5 GHz	10 GHz
A ...	0°.16	−0°.13	17^{h}43^{m}3	−28°50′	<0.5	~10	... (−2880)†	~−1000
A′ ...	0°.16	−0°.18	17 43.5	−28°52′	~1	≲0°.5	500–1000 (−200)†	...
B ...	~0°.15	0°.15 to 0°.5	~17 41.6	−28°40′	10–20	20–40	0–500	0–1000
C ...	~0°.14	−0°.4 to −0°.6	~17 44.8	−29°10′	5–10	20–30	−100 to −1000	−500 to −1000

* 5-GHz observations with the Effelsberg 100-m telescope HPBW 2′.4; 10 GHz with the NRO 45-m telescope, HPBW 2′.7.

† Values from VLA observations at a resolution of 20″ (Yusef-Zadeh et al. 1986).

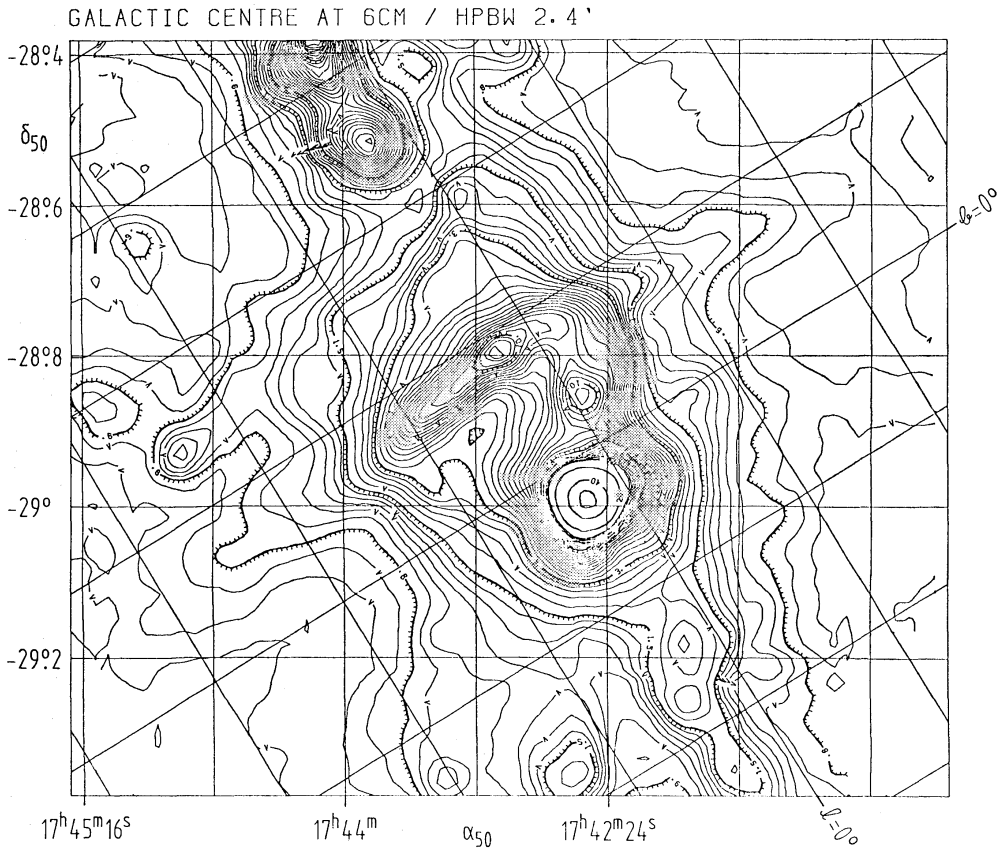

Fig. 1. Total intensity distribution of the galactic center region at 6-cm wavelength. Contours start from an arbitrary zero level in steps of 150 mJy/beam up to 1.5 Jy/beam, in steps of 300 mJy/beam up to 3 Jy/beam and further in steps of 500 mJy/beam up to 15 Jy/beam. The peak flux is about 63.0 Jy/beam. Coordinates are for α(1950) and δ(1950) with galactic coordinates superimposed in steps of 0°.2.

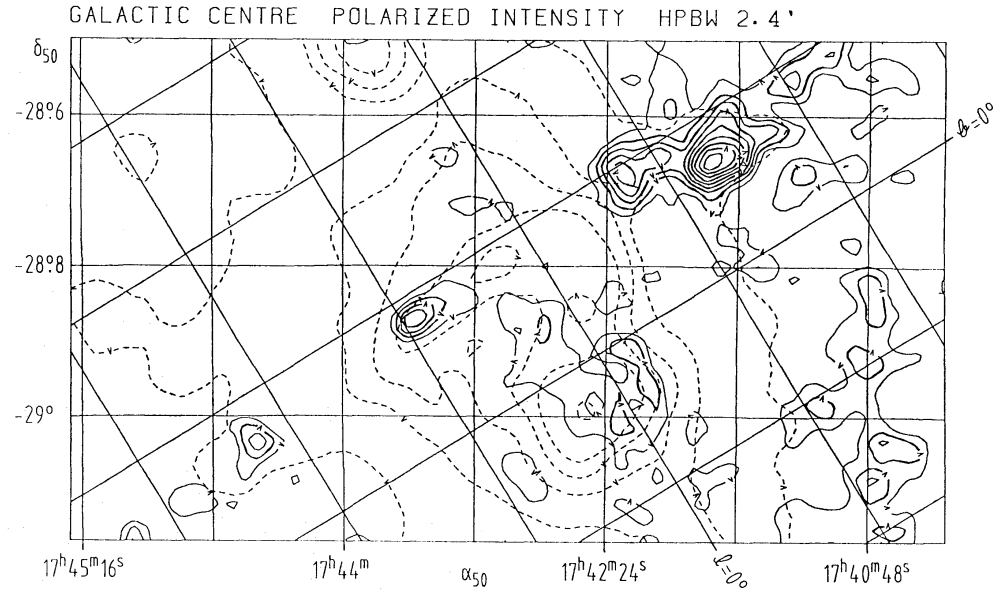

Fig. 2. Distribution of averaged polarized intensity of the four channels. Thick lines show polarized intensities in steps of 15 mJy/beam starting at 18 mJy/beam, that is 2.5 times the rms noise. Dashed lines represent some total intensity contours of figure 1.

superposed on the total intensity distribution as indicated with the dashed contours. Figures 3a–d show the individual results from the four channels. Significant polarization is detected in many regions including sources B and C (polarized plumes). Source A is very little polarized, whereas a compact region about 3′ south of source A is polarized by about 1%. VLA observations (Yusef-Zadeh et al. 1984) have shown a large, ordered magnetic structure at this position. We call this 5-GHz compact polarized source as source A′. Positions of the sources are shown in table 1.

Source B is detected at 10–20% level and source C at 5–10%. These polarization degrees are less than those observed at 10 GHz by a factor of two. The peak positions of the polarized intensity at 5 GHz in sources B and C are shifted by about 3′ from those at 10 GHz in the sense that they are farther away from the galactic plane than at 10 GHz. Polarization is also detected in a wide area east of Sgr A. Polarization within 3′ of Sgr A might still be due to the residual of the instrumental response, but polarization near the radio bridge is real.

3. RM Characteristics and Magnetic Fields

(i) Compact Polarized Sources A and A′

Figure 4 shows the RM distribution at 5 GHz as a function of the galactic latitude along the ridge containing the polarized features A, A′, B, and C at $l \cong 0^{\circ}.15$. Table 1 summarizes their polarization characteristics. A significant difference in RM behavior is found between 5 and 10 GHz for the compact sources A (10 GHz) and A′ (5 GHz). Source A is polarized at 10 GHz by $\sim 10\%$ and has a large negative RM of -1000 to -2000 rad m^{-2} (Inoue et al. 1984), but shows very little polarization at 5 GHz. On the contrary source A′ is polarized at 5 GHz by 1% and shows a large positive RM from 0 to 10^3 rad m^{-2}, but is not polarized at 10 GHz. A large negative RM (-2880 rad m^{-2}) at 5 GHz has been observed near source A with a higher resolution (20″) using VLA, while a smaller value (-200 rad m^{-2}) is reported near source A′ by the same observations (Yusef-Zadeh et al. 1986).

The proximity of sources A and A′ suggests their physical correspondence. Their anomalous RM behavior is far from allowing modeling yet. However, we offer the following possible interpretation.

If there exists internal Faraday rotation in the emitting region, the observed E vector is the superposition of E vectors from different Faraday depths and therefore with different position angles. Burn (1966) has shown that the observed polarization angle can then attain a maximum (or minimum) at a certain critical wavelength λ_c. This means that apparent (or observed) RM as defined by $d\phi/d\lambda^2$ becomes zero at λ_c and changes sign with wavelength across λ_c. The observed reversal of RM from 5 to 10 GHz for the compact sources A and A′ could then be accounted for, if this critical wavelength lies between 3 and 6 cm. This occurs for an internal Faraday depth of RM* $\sim 10^3$ rad m^{-2}, where RM* is defined through RM* $= K \int n_e B_{\parallel} dx$ (rad m^{-2}), K ($=0.81$) is a constant, n_e (cm^{-3}) is the thermal electron density, $B_{\parallel}$ (μG) is the line-of-sight field component, and x (pc) is the path length within the source.

The degree of polarization p changes also in a complicated manner (Burn 1966). The difference in position of sources A and A′ could be attributed to such a compli-

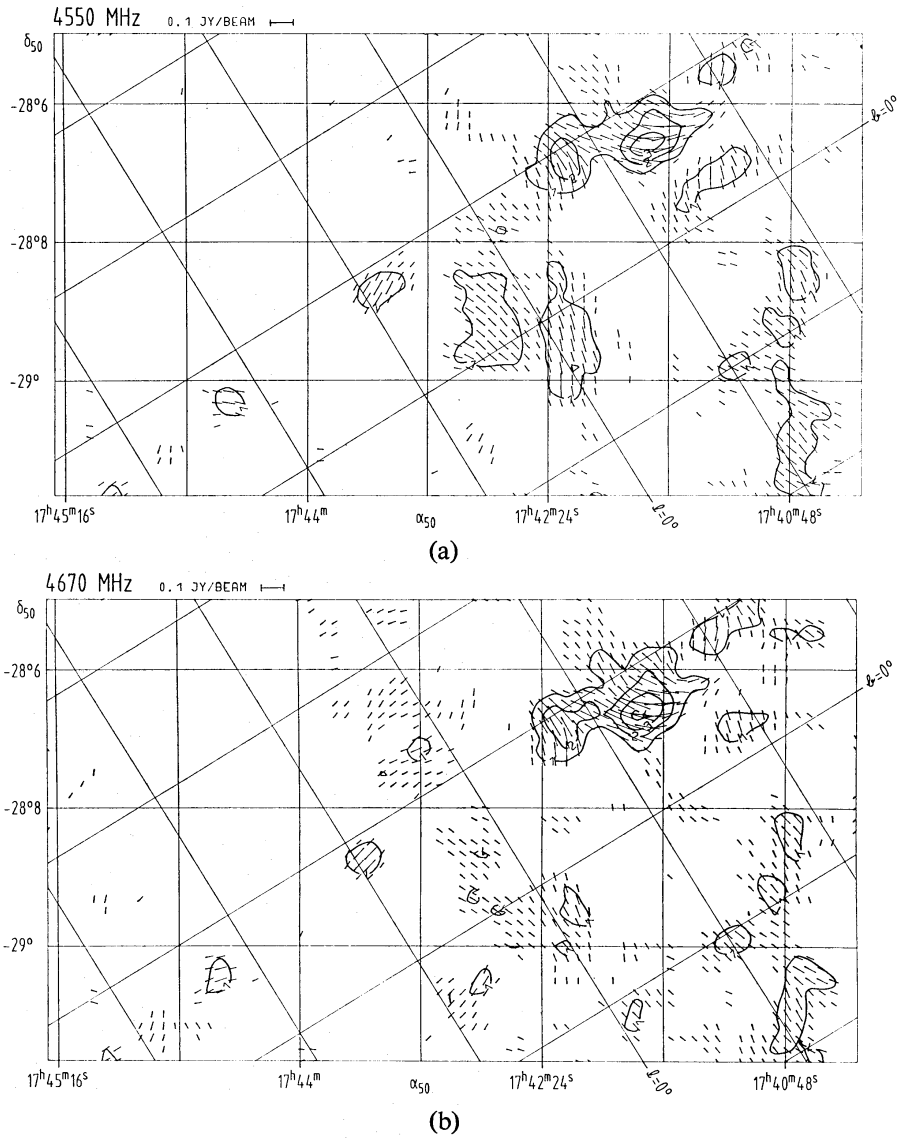

Fig. 3a and 3b. See the caption on the next page.

cated frequency dependence of the degree of polarization. Difference in RM within the finite beamwidth (2′.6 at 10 GHz and 2′.4 at 5 GHz) may also introduce further complications. It is too crude as yet to model the RM* behavior from the present data. We need definitely more observations at other frequencies, especially at higher frequencies.

(ii) RM Distribution across the Galactic Plane: Polarized Sources B and C (Plumes)

The absence of polarized emission at $-0°.1 \lesssim b \lesssim 0°.1$ and at $-0°.3 \lesssim b \lesssim -0°.2$ along the radio arc may be attributed to Faraday depolarization by a large internal rotation. Alternatively rapidly varying polarization angle within the beam width may also be responsible for the absence of polarized intensity in these regions. Sources A and A′ located in between these two depolarized regions may be the result of a "Faraday window," where the RM* changes steeply from negative to positive values through zero.

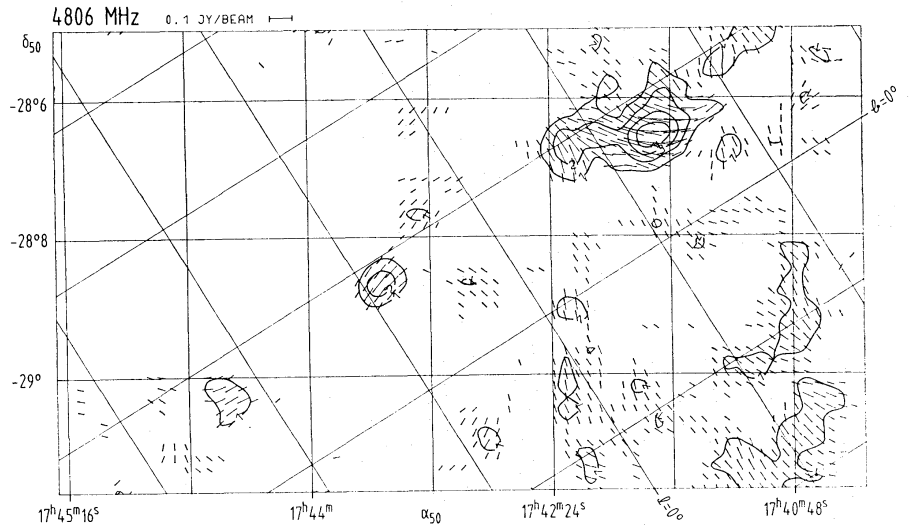

(c)

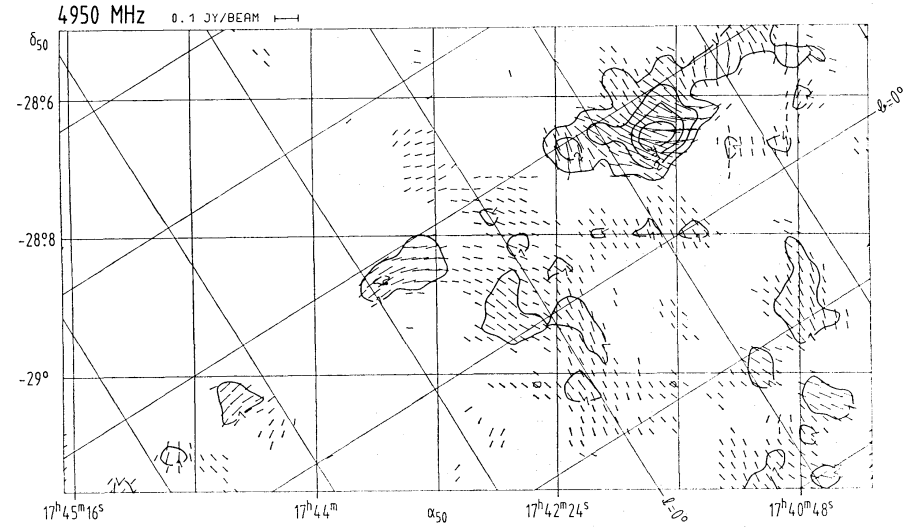

(d)

Fig. 3. Polarized intensity with superimposed polarization vectors in the E-field direction of four channels. Figures 3a–3d show the rerults for center frequencies of 4550, 4670, 4806, and 4950 MHz, respectively. The data are slightly smoothed to 2.′7 resolution. Contours are in steps of 38 mJy/beam. Vectors start at 25 mJy/beam.

The RM distribution at 5 GHz for the extended sources B and C (plumes) agrees with that at 10 GHz (Tsuboi et al. 1986). The RM in source B at $b>0°$ is positive and increases toward the galactic plane. In source C, the RM is negative and its absolute value increases again toward the galactic plane. The RM variations in B and C are antisymmetric with respect to the galactic plane (figure 4). This implies that the line-of-sight component of the magnetic field in the features has a reversal near the galactic plane and most likely near the compact source A or A′ where the Faraday window appears.

Tsuboi et al. (1986) have obtained intrinsic polarization angles along the features

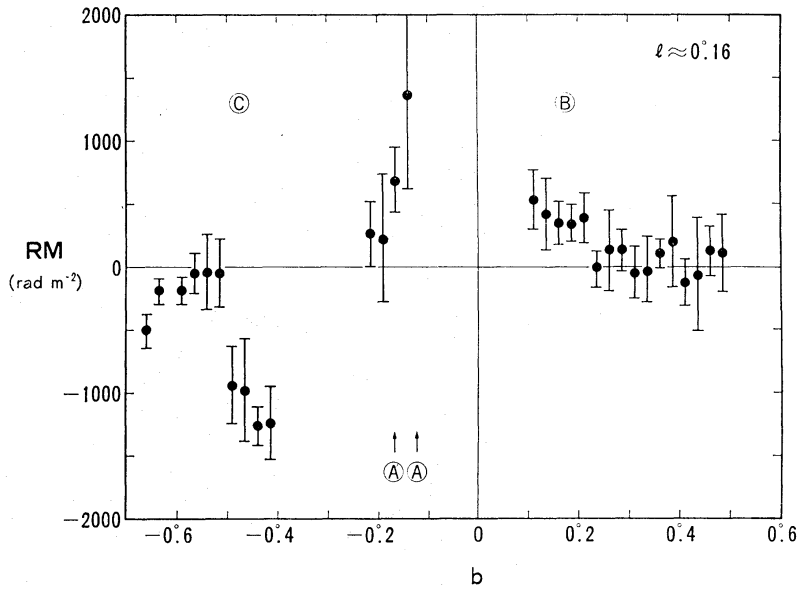

Fig. 4. The distribution of RM at 5 GHz along the polarized features A, A′, B, and C at $l=0^{\circ}.15$ across the galactic plane.

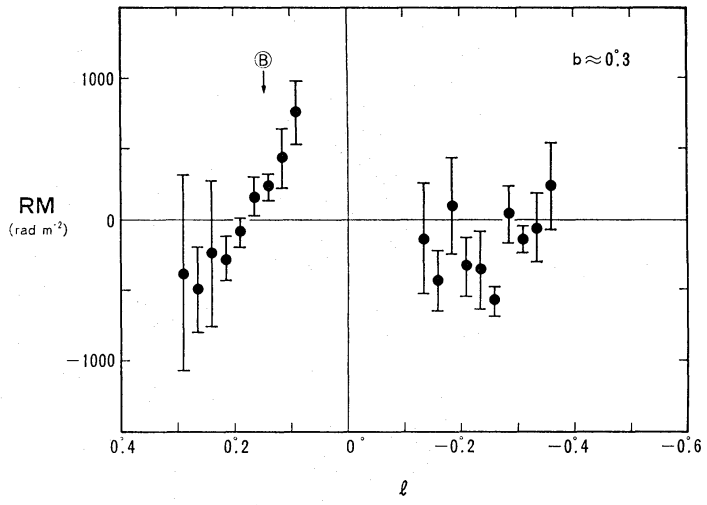

Fig. 5. The RM distribution along $b=0^{\circ}.3$ across the galactic rotation axis.

A, B, and C by correcting for the Faraday rotation at 10 GHz. They have shown that the transverse component of the magnetic field in the features is nearly perpendicular to the galactic plane. The VLA filaments found in the radio arc (Yusef-Zadeh et al. 1984) also indicate that the magnetic field runs parallel to the arc and perpendicular to the galactic plane.

(iii) RM Distribution across the Rotation Axis

The variation of RM as a function of the galactic longitude close to the galactic plane across the rotation axis of the Galaxy indicates a characteristic magnetic field configuration parallel to the galactic disk (Sofue et al. 1986). Figure 5 shows a plot of RM obtained at 5 GHz as a function of the longitude at a fixed latitude, $b\cong 0^{\circ}.3$. It is remarkable that the RM varies steeply across the northern polarized fea-

ture B, from RM$\simeq$0 at $l\sim0^\circ.2$ to almost 10^3 rad m^{-2} at $l\sim0^\circ.1$. On the opposite side of the rotation axis we have smaller variations. The RM increases from negative values around $l=-0^\circ.1$ to $-0^\circ.2$, to about zero at $l\cong-0^\circ.3$. The RM variation seems to be antisymmetric with respect to $l\cong-0^\circ.05$. Such an antisymmetric variation of RM across the rotation axis may indicate that there exists a ringlike (or toroidal) magnetic field (Sofue et al. 1986). The field direction in the ring is toward the observer (RM positive) at positive longitude and away from the observer on the opposite side.

(iv) Large-Scale Magnetic Field

On the basis of the observed characteristics of RM at 5 and 10 GHz we propose the following view about the large-scale magnetic field in the central 100 pc of the Galaxy, though still not conclusive enough for large errors, especially at $l<0^\circ$.

There exists a poloidal magnetic field running across the galactic plane perpendicular to it. The field is twisted by the rotation of the disk, as it rotates faster than the halo gas to which the poloidal field is anchored. The twist produces a toroidal field component, whose direction is opposite in the upper and lower sides of the galactic plane. Figure 6 illustrates the field configuration proposed here. This type of configuration was already suggested by a magnetic-twisted acceleration model of the Ω-shaped galactic center lobe by Uchida et al. (1985).

A large-scale poloidal field in the galactic center region may be readily argued on the basis of the "primordial" origin hypothesis of the galactic magnetic field (Piddington 1969). Sofue et al. (1986) have shown that most spiral galaxies possess a bisymmetric open spiral magnetic field in their disks. They argue that this configuration results from winding up of an intergalactic magnetic field to a disk of a protogalaxy when the galaxy formed. In the central region the wound-up field by a strong differential rotation can easily reconnect through the turbulent diffusion (Sawa and

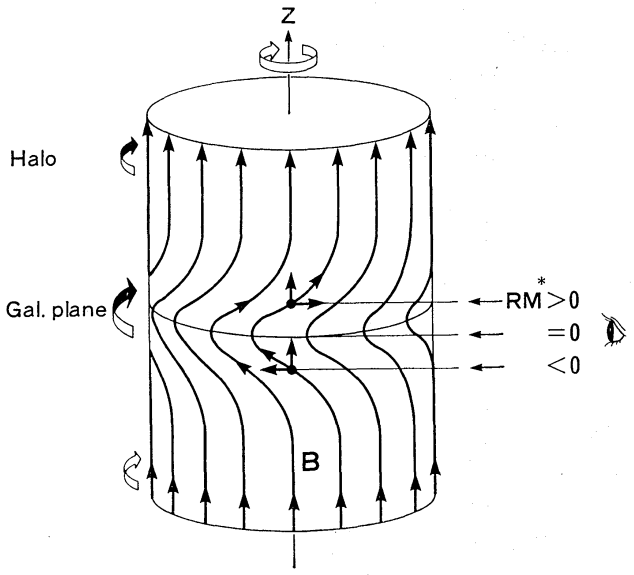

Fig. 6. Schematic sketch of a possible large-scale poloidal magnetic field twisted by the disk rotation.

Fujimoto 1986). However, if there existed a poloidal component, it can never reconnect or diffuse away from the disk, for the diffusion time radially crossing the galactic disk is much longer than the Hubble time scale. Thus the poloidal field is more gathered toward the center by an accreting process of the disk gas, and is conserved for the entire life time of the galaxy. The poloidal field in the center of our Galaxy may thus be attributed to such a primordial process. In fact our Galaxy has been shown to possess a bisymmetric spiral field indicative of the primordial origin (Sofue et al. 1986).

Although this large-scale field configuration is a natural consequence of the observed RM distribution, there remains a question why the polarized features, A, A′, B, and C, alone are bright compared to the surrounding regions. This may be answered if we consider the features as a "synchrotron tube" illuminated by high-energy electrons that are accelerated in the radio arc when the arc is encountered by a jet from the nucleus through the radio bridge.

The strength of magnetic field along the radio arc and its high-latitude extensions is derived as roughly 30 μG from an equipartition assumption between the field energy and cosmic-ray energy densities (e.g., Moffet 1975). About the same field strength has been derived from the RM value at 10 GHz (Inoue et al. 1984). If the poloidal field is of primordial origin from an intergalactic field, a frozen-in field to the gaseous component in the nuclear disk can be evaluated. Suppose that a magnetic field perpendicular to the galactic plane of strength B_{z0} was trapped in the disk of gas density n. Then the present poloidal field strength is given by $B_z=B_{z0}(n/n_0)^{2/3}$, where n_0 is the intergalactic gas density. From the total amount of gaseous content of $\sim 10^8\,M_\odot$ in a few hundred parsec space of the galactic center (e.g., Scoville 1980) we have a mean $n\sim 100$ cm^{-3}. An intergalactic field of $\sim 10^{-9}$ G has been suggested for a gas density of $n_0\sim 10^{-5}$ cm^{-3} (Sofue et al. 1979). Then we obtain $B_z\approx 50\,\mu$G, in agreement with the observed field strength.

(v) RM Distribution across the Radio Bridge and Its Magnetic Field

Significant polarization is detected in the region surrounding the radio bridge, the region of strong radio emission which connects the radio arc with Srg A. On the other hand no polarization was recorded in the brightest part of the bridge. There appears to exist an anticorrelation between the total intensity and polarized intensity on the bridge. A distribution of RM across the radio bridge has been obtained for the region where the polarization exceeded 25-mK level. Figure 7 shows the RM distribution at (a) Decl.(1950)$=-28°52'$ and (b) $-28°55'$ as a function of right ascension. The plot shows that the RM variation along the two different sections, separated by more than a beamwidth, has almost identical behavior.

The rotation measure has a deep minimum across the bridge center. The minimum value along Decl.$=-28°52'$, crossing the highest intensity complex of the bridge, is as small as -1000 rad m^{-2}, and almost the same value is obtained at Decl.$=-28°55'$. At the bridge center, where RM is expected to be smaller than -10^3 rad m^{-2}, we have no polarization detected. The coherent increase in |RM| toward the bridge center and the depolarization at the brightest part may indicate a strong magnetic field along the bridge and a large internal Faraday rotation.

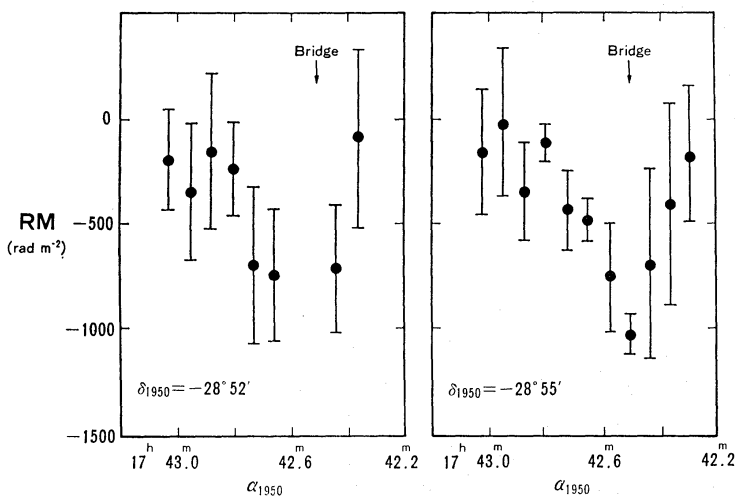

Fig. 7. Distributions of RM across the radio bridge at (a) Decl. = −28°52′ and (b) −28°55′. The coherent variation shows that the magnetic field is highly ordered in the bridge.

Pauls et al. (1976) have examined the thermal characteristics of the bridge using recombination line observations. They showed that the bridge involves ionized hydrogen gas of density 100–400 cm^{-3}. The flat radio spectrum of the bridge (e.g., Sofue 1985) is also suggestive of its thermal nature. Nevertheless, if one looks at the complex, anomalous filamentary structure on the VLA map (Yusef-Zadeh et al. 1984), one might expect a strong influence of a magnetic field on the bridge. In fact, our RM observations confirm the magneto-ionic characteristics of the radio bridge. The regular RM variation (figure 7) suggests an ordered magnetic field, most likely aligned along the bridge. From the largest |RM| in figure 7 and the corresponding thermal electron density from Pauls et al. (1976), $n_e \sim 10^2$ cm^{-3}, we obtain a magnetic field strength of about 10 μG on the edge of the bridge for an assumed path length of 2 pc. In the central part of the bridge the field strength will be larger, and an estimate of $B \sim 10^2$ μG has been suggested on the assumption of a balance between the magnetic energy and the internal thermal energy of gas in the bridge. In this case the internal Faraday depth could be as large as RM* $\sim 10^4$ rad m^{-2}, which is consistent with the observed depolarization.

Finally we would like to know where the polarized synchrotron emission near the bridge comes from. One possibility is that the emission is due to background nonthermal emission which suffers from Faraday depolarization when penetrating the bridge and its neighborhood. The other is that the bridge itself emits synchrotron emission, or a mixture of thermal and nonthermal radiations. The depolarization on the brightest parts of the bridge implies that it is located at the nearer side of the background nonthermal emission. If the nonthermal emission is mainly due to the halo of Sgr A, the bridge is approaching toward us from Sgr A and the negative RM indicates that the field there is away from the observer or runs toward Sgr A.

4. Summary

Four-channel, narrow-band polarimetric observations at 5 GHz have been done

with the Effelsberg 100-m telescope for the region surrounding the galactic center, the radio bridge, and the arc. Our results can be summarized as follows:

(1) The compact sources A (10 GHz) and A′ (5 GHz) show drastically different RM characteristics, and their positions are significantly different, although their proximity suggests a physical connection. They show a very complicated RM dependence on frequency, which indicates a large internal Faraday effect near a "Faraday window" through a reversal point of the line-of-sight field component.

(2) Polarization structures at 5 GHz for the polarized plumes (sources B and C) are basically consistent with those obtained at 10 GHz. The large-scale RM attains large positive values for $b>0°$ and negative for $b<0°$, indicating a field reversal near the galactic plane.

(3) RM distribution across the galactic rotation axis for $b>0°$ shows an antisymmetric variation with respect to the axis. This indicates the existence of a toroidal field component.

(4) The global RM distribution suggests that a large-scale poloidal magnetic field exists in the central 100 pc of the Galaxy. The poloidal field is twisted by the disk rotation which yields the toroidal component in the upper and lower sides of the galactic plane (figure 6).

(5) Significant polarization has been detected in the region surrounding the radio bridge, showing for the first time the magneto-ionic character of the bridge. A strong magnetic field of $B\sim 10$–100 μG is suggested.

The authors are grateful to Professor R. Wielebinski for discussions and encouragement. This work was done as a part of the collaborative research program between NRO and MPIfR under the financial support of the Japan Society for the Promotion of Science and of the Alexander von Humbolt-Stiftung.

References

Brown, R. L., and Liszt, H. S. 1984, *Ann. Rev. Astron. Astrophys.*, **22**, 223.
Burn, B. J. 1966, *Monthly Notices Roy. Astron. Soc.*, **133**, 67.
Inoue, M., Takahashi, T., Tabara, H., Kato, T., and Tsuboi, M. 1984, *Publ. Astron. Soc. Japan*, **36**, 633.
Moffet, A. T. 1975, in *Galaxies and the Universe*, ed. A. Sandage, M. Sandage, and J. Kristian (University of Chicago Press, Chicago), chap. 7.
Pauls, T., Donnes, D., Mazger, P. G., and Churchwell, E. 1976, *Astron. Astrophys.*, **46**, 407.
Piddington, J. H. 1969, *Cosmic Electrodynamics* (John Wiley and Sons Inc., New York), chap. 12.
Sawa, T., and Fujimoto, M. 1986, *Publ. Astron. Soc. Japan*, **38**, 133.
Scoville, N. Z. 1980, in *Giant Molecular Clouds in the Galaxy*, ed. P. M. Solomon and M. G. Edmunds (Pergamon Press, Oxford), p. 123.
Seiradakis, J. H., Lasenby, A. N., Yusef-Zadeh, F., Wielebinski, R., and Klein, U. 1985, *Nature*, **317**, 697.
Sofue, Y. 1985, *Publ. Astron. Soc. Japan*, **37**, 697.
Sofue, Y,, Fujimoto, M., and Kawabata, K. 1979, *Publ. Astron. Soc. Japan*, **31**, 125.
Sofue, Y., Fujimoto, M., and Wielebinski, R. 1986, *Ann. Rev. Astron. Astrophys.*, **28**, 459.
Sofue, Y., and Handa, T. 1984, *Nature*, **310**, 568.
Tsuboi, M., Inoue, M., Handa, T., Tabara, H., and Kato, T. 1985, *Publ. Astron. Soc. Japan*, **37**, 359.
Tsuboi, M., Inoue, M., Handa, T., Tabara, H., Kato, T., Sofue, Y., and Kaifu, N. 1986, *Astron. J.*, **92**, 818.

Uchida, Y., Shibata, K., and Sofue, Y. 1985, *Nature*, **317**, 699.
Yusef-Zadeh, F., Morris, M., and Chance, D. 1984, *Nature*, **310**, 557.
Yusef-Zadeh, F., Morris, M., Slee, O. B., and Nelson, G. J. 1986, *Astrophys. J.*, **310**, 689.